

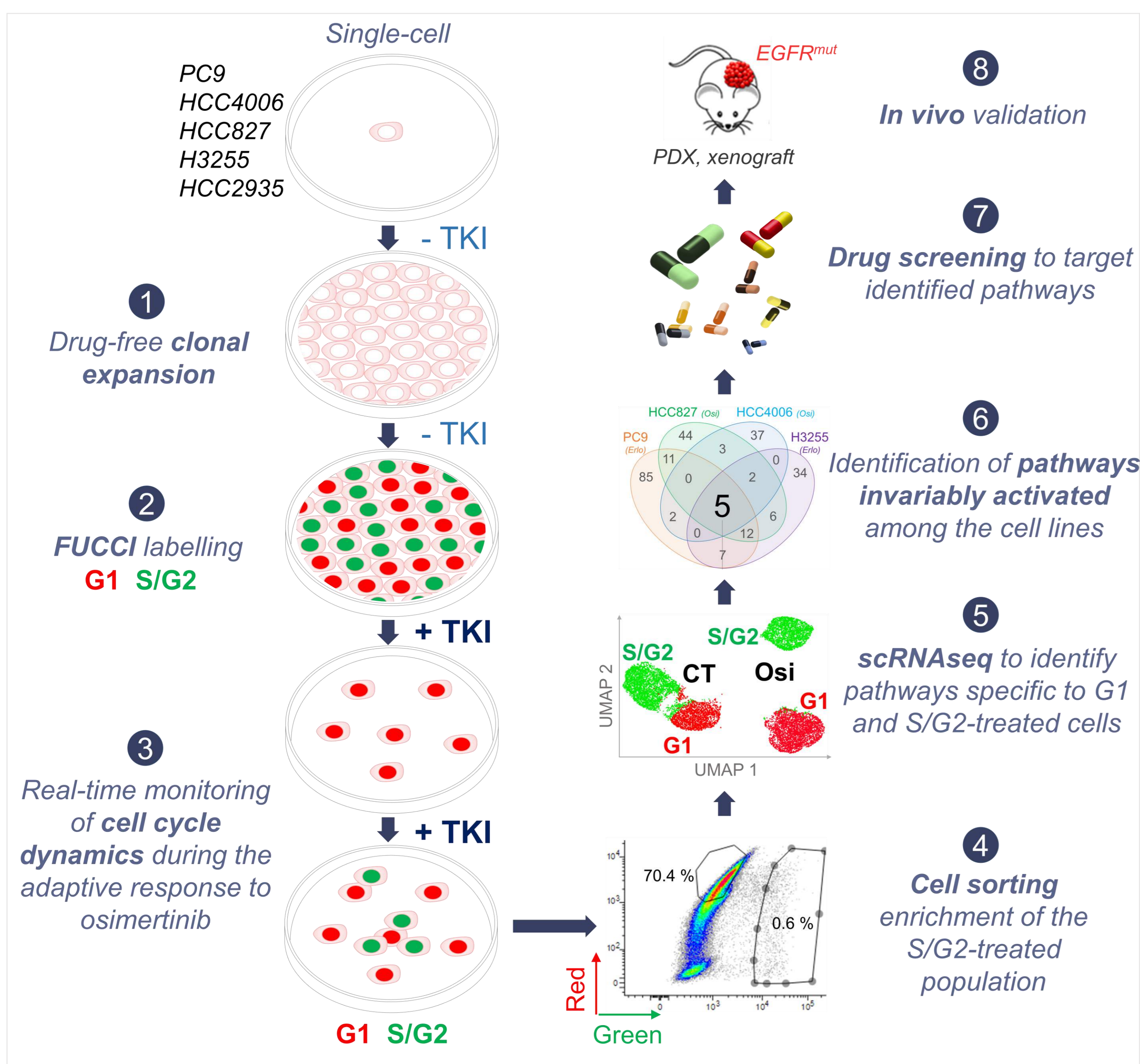
Sarah Figarol^{1,2}, Célia Delahaye¹, Rémi Gence¹, Raghda Asslan¹, Sandra Pagano^{1,2}, Claudine Tardy¹, Jacques Colinge⁵, Jean-Philippe Villemin⁵, Antonio Maraver⁵, Isabelle Lajoie-Mazenc^{1,2}, Estelle Clermont^{1,3}, Anne Casanova³, Anne Pradines^{1,3}, Julien Mazières^{1,2,4}, Olivier Calvayrac¹, Gilles Favre^{1,2,3}.

¹ Cancer Research Center of Toulouse, INSERM U1037/CNRS ERL5294/UPS, Toulouse, France; ² University Paul Sabatier, Toulouse, France; ³ Institut Claudius Regaud, Institut Universitaire du Cancer de Toulouse-Oncopole, Laboratory of Medical Biology and Oncogenetics, Toulouse, France; ⁴ Toulouse University Hospital, France; ⁵ Cancer Research Institute of Montpellier, INSERM U1194, Montpellier University, ICM, Montpellier, France

Background

Drug-tolerant “dormant” cells (DTC) have emerged as one of the major non-genetic mechanisms driving resistance to targeted therapy in lung cancer¹⁻⁴, although the sequence of events leading to entry and exit from dormancy remains poorly described. Here, we provide a step-by-step phenotypic and molecular characterization of the different processes involved during the adaptive response to osimertinib using several EGFR-mutated lung cancer models. This strategy led to the identification of a common vulnerability of drug-tolerant cells which could be efficiently and safely targeted by a clinical stage drug.

Methods



A panel of EGFR-mutated NSCLC cell lines was subcloned to minimize/avoid the presence of potential pre-existing resistant cells (1), and transduced with the FUCCI (fluorescence ubiquitination cell cycle indicator) system (2) to perform real-time monitoring of the cell cycle dynamics in response to 1 μM erlotinib or osimertinib (3). G1 (red) and S/G2 (green) cells were sorted during the early stage of the adaptive response to EGFR-TKI (4) and scRNAseq experiments were performed to identify the molecular mechanisms underlying entry and exit from dormancy (5). GSEA analysis was performed to determine molecular pathways invariably activated among the cell lines (6), and *in vitro* drug screening was conducted to target identified pathways (7). The most relevant combinations were validated *in vivo* using EGFR-mutated NSCLC xenografts and PDX (Patient-Derived Xenografts) (8).

Conclusions

We report that adaptive response to osimertinib is a highly dynamic process which invariably involves a dedifferentiation process through an alveolar type-1 phenotype with contractile features. Using a screen of Rho/ROCK pathway inhibitors, we found that tipifarnib, a clinically active farnesyltransferase inhibitor, efficiently and durably prevented relapse to osimertinib *in vitro* and *in vivo* by inducing an ATF4-dependent apoptotic response, with no evidence of toxicity in mice. Collectively, our data strongly support the use of tipifarnib in combination with osimertinib in the clinic to effectively and durably prevent relapse.

Results

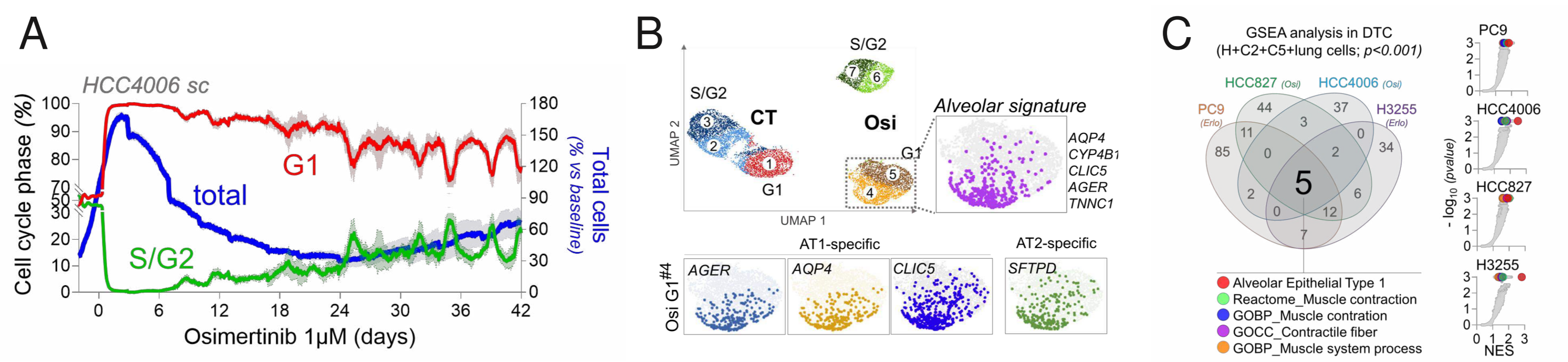


Figure 1. Osimertinib resistance emerges from an alveolar-like phenotype with contractile features
A. Percentage of total cells (blue), S/G2 (green) or G1 (red) population of HCC4006 subclonal cells during the adaptive response to 1 μM osimertinib
B. UMAP representation of the different populations of untreated and osimertinib-treated HCC4006 clonal cells. The alveolar signature is highlighted.
C. Left: Venn diagram comparing the significantly enriched pathways (p<0.001) in erlotinib- or osimertinib-derived drug-tolerant cells. Right: Volcano plots of the pathways enriched in indicated EGFR-TKI-treated DTC

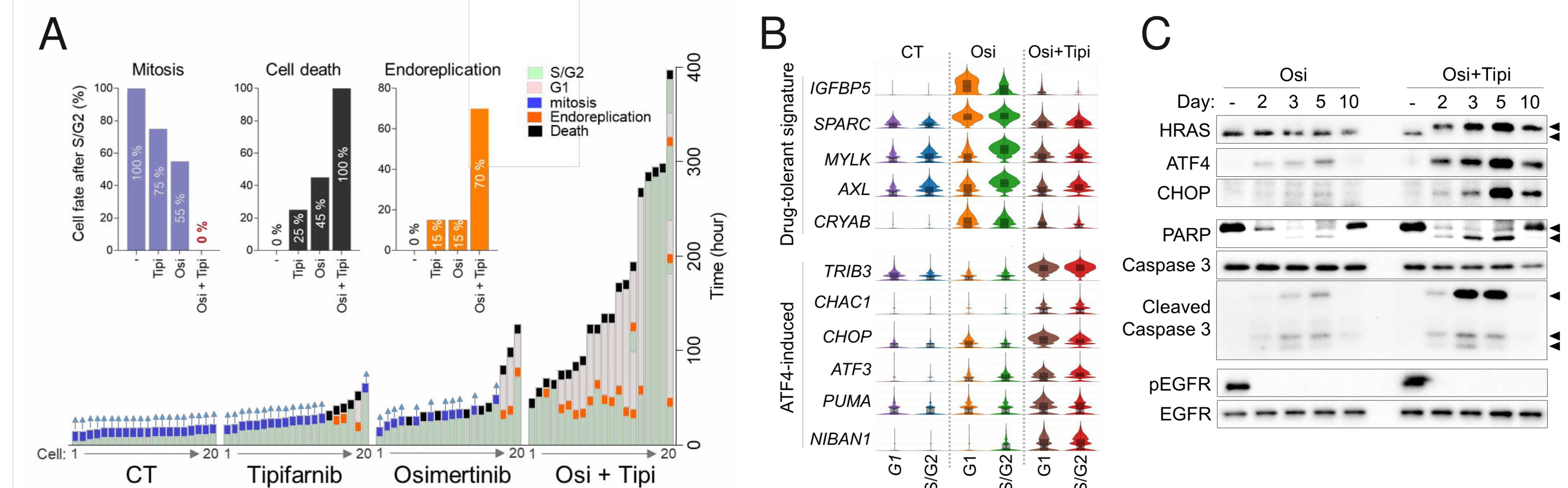


Figure 4. Osimertinib+Tipifarnib treatment impairs mitosis and induces an integrated stress response (ISR)-mediated apoptotic pathway
A. Cell fate after entry in S/G2 of HCC4006 clonal cells in response to osimertinib (1 μM), tipifarnib (1 μM) or the combo.
B. Drug-tolerant-specific (top) and ATF4-induced (bottom) genes regulated by 1 μM tipifarnib in combination with 1 μM osimertinib
C. Protein expression by Western blot of ATF4, CHOP, HRAS, PARP, total and cleaved caspase 3, total and pEGFR in response to osimertinib (1 μM) or osimertinib (1 μM) + tipifarnib (1 μM).

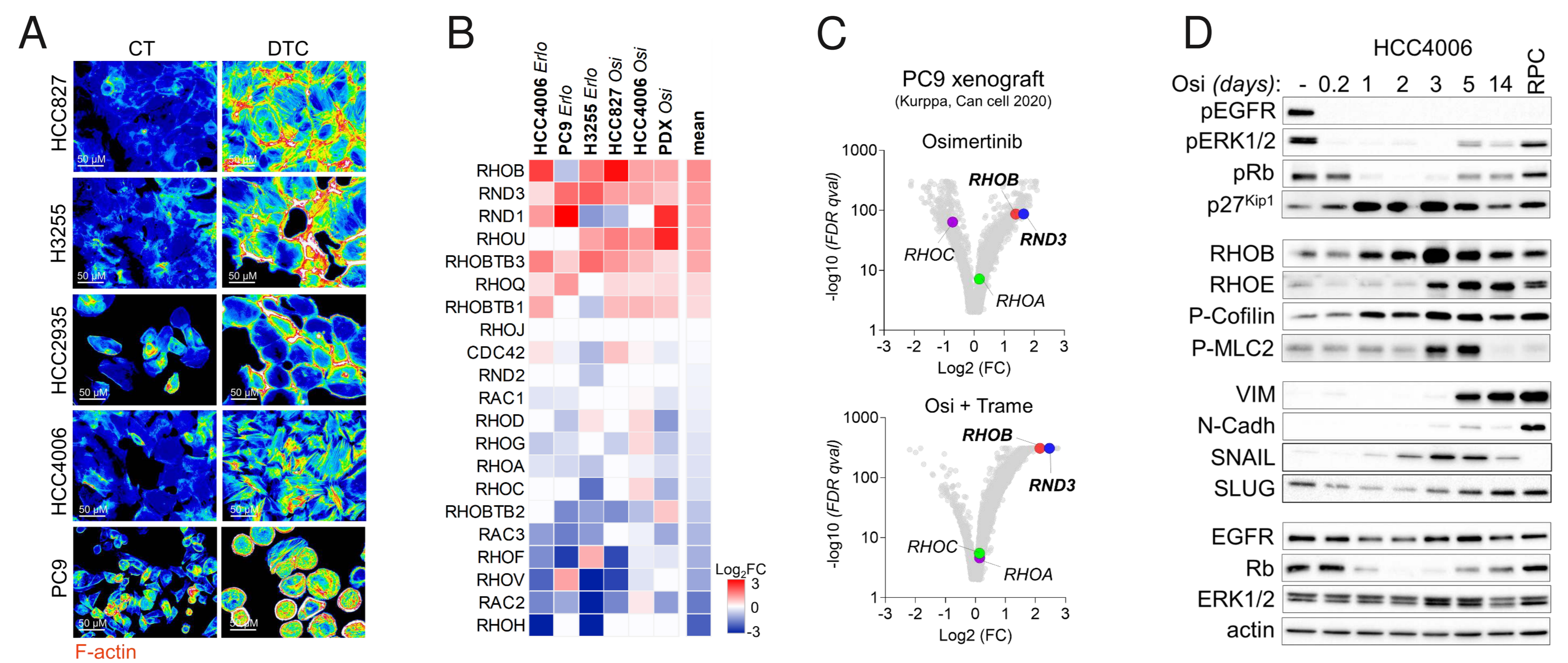


Figure 2. Drug-tolerant cells display cytoskeletal remodeling and Rho/ROCK pathway activation
A. Phalloidin F-actin staining of untreated and osimertinib-derived DTC.
B. Differential mRNA expression of the 21 known Rho-GTPases in several *in vitro* and *in vivo* models of EGFR-TKI-derived DTC.
C. Volcano plot of the differentially expressed genes in osimertinib- (up) or osimertinib+trametinib- (down) treated PC9 xenografts. Data were obtained from a scRNAseq published by Pasi Jänne's lab (Kurppa *et al.* *Cancer Cell*, 2020)
D. Protein expression by western blot of proteins related to EGFR pathway, cell contractility, EMT, cell cycle and RhoGTPases in response to 1 μM osimertinib
 RPC= resistant proliferative clone

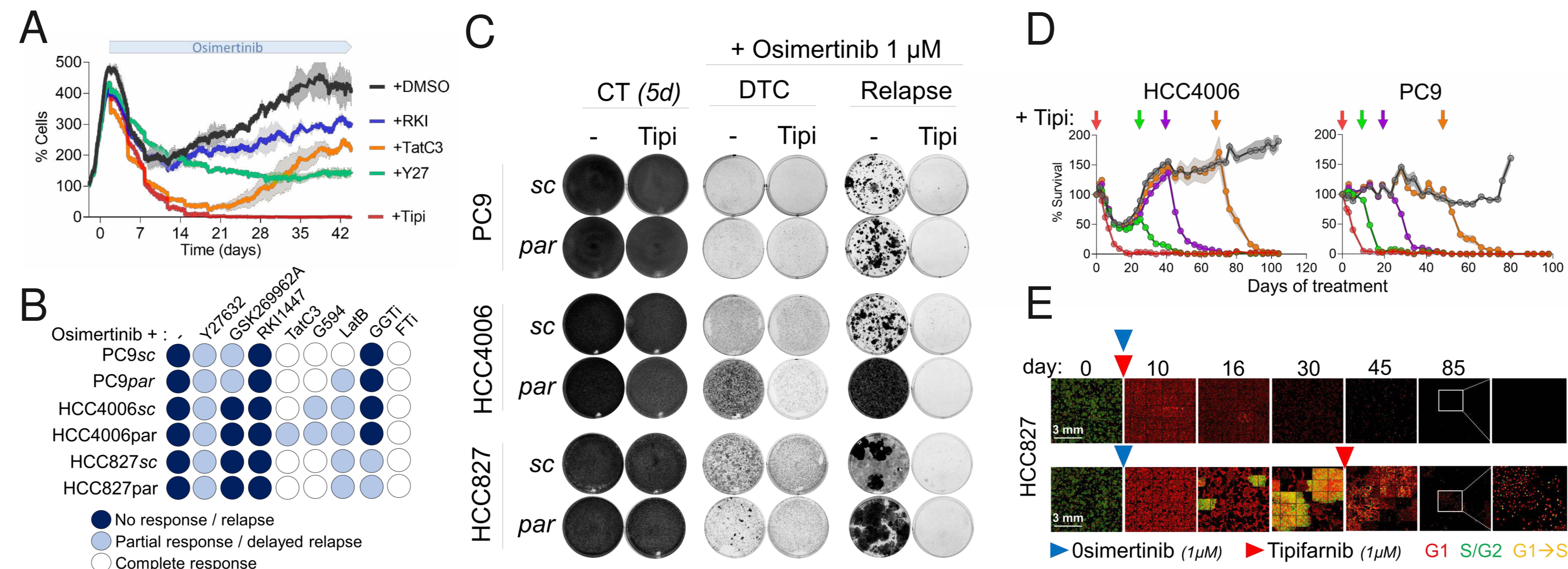


Figure 3. The farnesyltransferase inhibitor tipifarnib prevents relapse to osimertinib *in vitro*
A. Cell survival (%) of HCC4006 parental cells during osimertinib treatment (1 μM) alone or in combination with ROCK inhibitors (RKI, RKI1474 and Y27, Y27632), RHOA/B/C inhibitor (TatC3) or farnesyl-transferase inhibitor (Tipi, tipifarnib).
B. Drug screening of RHO/ROCK inhibitors in combination with 1 μM osimertinib. Deep blue: no response/relapse, light blue: partial/delayed response, white: complete response.
C. Crystal violet staining of clonal and parental cells treated with 1 μM osimertinib (1 μM) alone or in combination with 1 μM tipifarnib.
D. Cell survival (%) of HCC4006 and PC9 cells during osimertinib treatment (1 μM) with or without tipifarnib (1 μM) added at several timepoints.
E. Incucyte imaging of FUCCI-labeled HCC827 cells in response to osimertinib (1 μM) +/- tipifarnib (1 μM). Arrows indicate treatment start (blue: Osi, red: tipi).

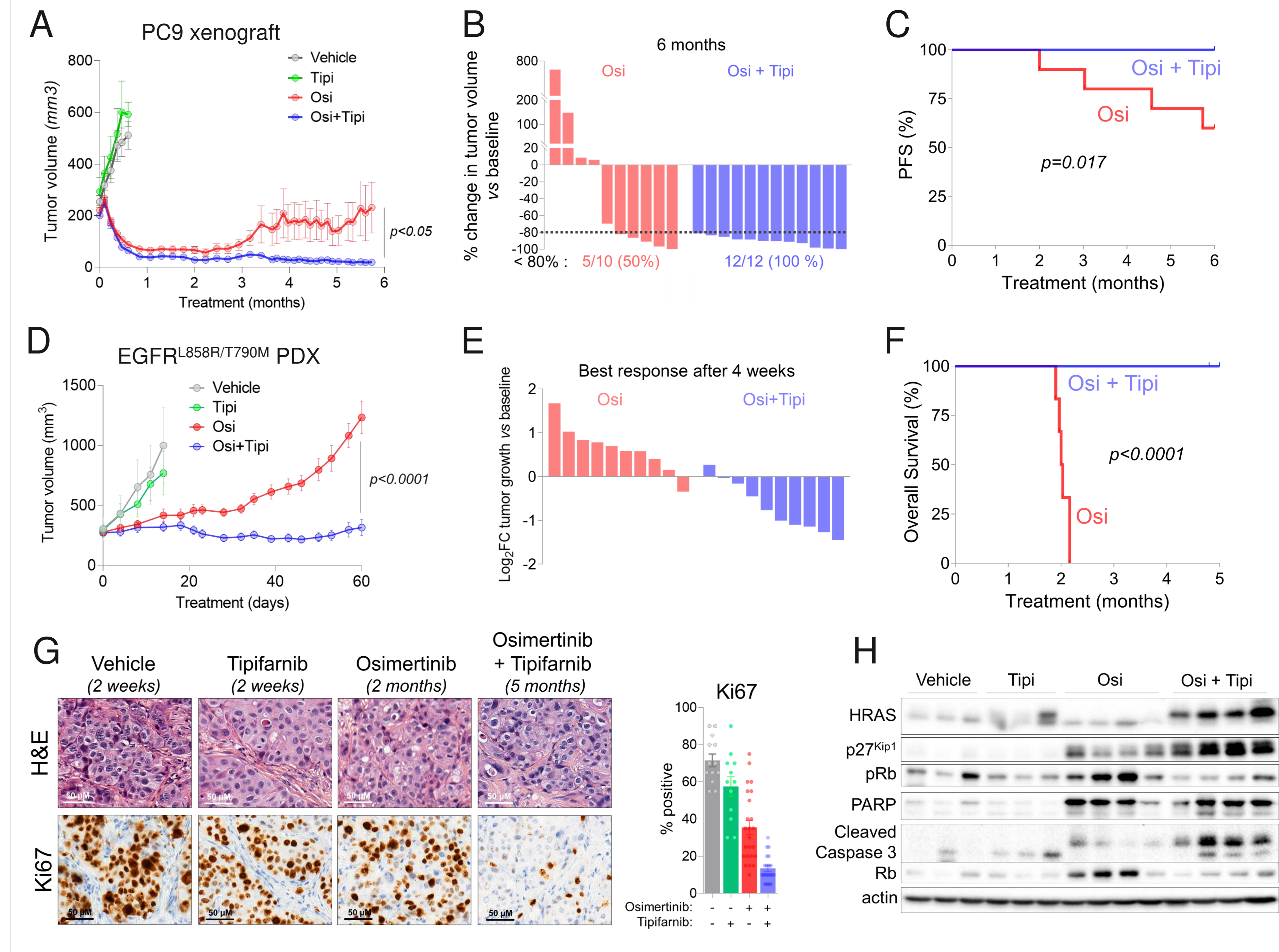


Figure 5. Tipifarnib prevents relapse to EGFR-TKI *in vivo*
A. Mean tumor volume of PC9 xenografts treated 5 d/w with vehicle (n=6), Tipifarnib (Tipi, 80 mg/kg, *b.i.d.*; n=6), Osimertinib (Osi, 5 mg/kg, *q.d.*; n=10), or by the combo (Osi + Tipi; n=12). Graph represents mean ± SEM.
B. Change in tumor volume versus baseline of PC9 xenografts after 6 months of treatment with Osimertinib or a combination of Osimertinib and Tipifarnib
C. Progression-free survival (PFS) of PC9 xenograft mice treated with Osimertinib or Osimertinib+Tipifarnib. P-value was determined by log-rank Mantel-Cox test.
D. Mean tumor volume of a PDX model of EGFR^{L858R/T790M} NSCLC treated 5 d/w with vehicle (n=4), tipifarnib (Tipi, 80 mg/kg, *b.i.d.*; n=5), Osimertinib (Osi, 5 mg/kg, *q.d.*; n=10), or by the combo (Osi + Tipi; n=10). Graph represents mean ± SEM.
E. Log2 fold change of the PDX growth compared to baseline after 60 days of treatment with Osimertinib or Osimertinib + Tipifarnib.
F. Overall survival (OS) of EGFR^{L858R/T790M} PDX mice treated with Osimertinib or Osimertinib + Tipifarnib. The graph is the result of one cohort of mice with n = 6 mice in both arms. P-value was determined by log-rank Mantel-Cox test.
G. Left: Representative images of Hematoxylin and Eosin (H&E) (top) and Ki67 (bottom) IHC stainings of PDX tumors collected after 2 weeks, 2 months and 5 months of treatment with Tipifarnib, Osimertinib Osimertinib + Tipifarnib, respectively. Right: Quantification of Ki67 IHC scores.
H. Protein expression by western blot of HRAS, p27^{Kip1}, total and pRb (retinoblastoma), PARP and cleaved caspase 3 in lysates from individual PDX harvested after 2 weeks, 2 months and 5 months of treatment with Tipifarnib, Osimertinib or Osimertinib + Tipifarnib, respectively.